Magmatic Plumbing System of Young, Lunar Mare Basalt: Northwest Africa (NWA) 8632. A. Madera[1], J. Gross[1,2,3,4], A.L. Fagan[5], M. Righter[6], T.M. Erickson[4,7] [1]Rutgers, The State University of New Jersey, Piscataway, NJ (am1505@eps.rutgers.edu); [2]American Museum of Natural History, New York, NY 10024; [3]Lunar and Planetary Institute, Houston, TX 77058; [4]Astromaterials Research and Exploration Science division, NASA JSC, Houston, TX, 77058; [5]Western Carolina University, Cullowhee, NC 28723, [6]University of Houston, TX. [7]Jacobs-JETS contract, Houston, TX, 77058.

Introduction: Lunar mare basalt volcanism peaked between 3.6-3.8 Ga, as evidenced by the Apollo and Luna basalts and crater counting chronometry. However, basaltic volcanism appears to have extended to ~1.0 Ga based on remote sensing observations [1]. Periodic pulses of post-peak volcanism are reflected by the youngest ages of the Apollo basalts (3.3-3.1 Ga), young lunar basaltic meteorites (3.0-2.7 Ga), and CNSA Chang'e 5 (CE5) samples (~2.0 Ga) [2]. Models of the Moon's thermal evolution with respect to its size suggest late-lunar volcanic activity is contradictory to the hypothesized cooling of the lunar mantle [3]. Furthermore, the drivers and conditions of late basaltic volcanism remain unclear. The limited available samples (i.e., young basaltic meteorites and CE5) provide critical views of the Moon's thermal history post-peak mare basalt production and are essential to placing constraints on its drivers and dynamics. Meteorite Northwest Africa (NWA) 8632 is an unbrecciated, lunar basalt with a $^{40}Ar/^{39}Ar$ age of 2.877 ± 0.034 Ga [4], and thus, is an important sample of post-peak lunar volcanism. Recent work [5] has shown NWA 8632 hosts pronounced sector-zoning of minor elements in euhedral clinopyroxenes that, coupled with texture and chemistry, are useful for constraining the crystallization kinetics of this sample. In this study, we place constraints on the potential parent magma plumbing system of NWA 8632 using bulk-rock chemistry, mineral chemistry, and textural analyses, which we then compare to other young mare basaltic meteorites of similar age and composition.

Methods: Quantitative point analyses of NWA 8632 and qualitative X-ray element maps were collected using the JEOL 8200 electron microprobe at Rutgers University (RU). Bulk-rock major and trace elements were collected using the Agilent 8800 Triple Quad inductively coupled plasma (ICP-QQQ) mass spectrometer and Agilent 723 ICP optical emission spectrometer (OES) at the University of Houston (UH).

Results: NWA 8632 is a porphyritic basalt (Fig. 1A) composed of olivine (22.4%), clinopyroxene (37.7%), and chromite (0.8%) set in a fine-grained groundmass (39.1%) of clinopyroxene, fayalitic olivine, and ilmenite. Accessory phases within the groundmass are comprised of sulfides, phosphates, and Fe-Ni metal. Olivine and pyroxenes each occur in three groups based on texture and size. *Olivine*: Group 1a- euhedral to subhedral macrocrysts (up to ~2.00 mm in length); Group 1b- euhedral to subhedral phenocrysts (up to ~350 µm in length); Group 1c- skeletal microcrysts (~ <100 µm in length). *Pyroxene*: Group 2a- Large euhedral phenocrysts (up to 665 µm in length); Group 2b- elongated, skeletal grains (up ~1 mm in length); Group 2c- dendritic pyroxenes within the groundmass (<10 µm). Within the olivines and pyroxenes groups, three distinct zonation patterns are observed. Both minerals exhibit normal-zoning of major elements (Fig. 1B) from core to rim. In addition, group 1b and 1c olivine exhibit thin-band phosphorus (P) oscillatory zoning (Fig. 1C) [4]; Group 2a pyroxenes exhibit sector-zoning (Fig. 1D) with "hour-glass" regions [5] depleted in minor elements Ti, Al, V, and Cr, with some also exhibiting oscillatory zoning (Fig. 1E) of minor elements Cr > Ti > and Al (in order of zoning visibility) within the core to mantle regions.

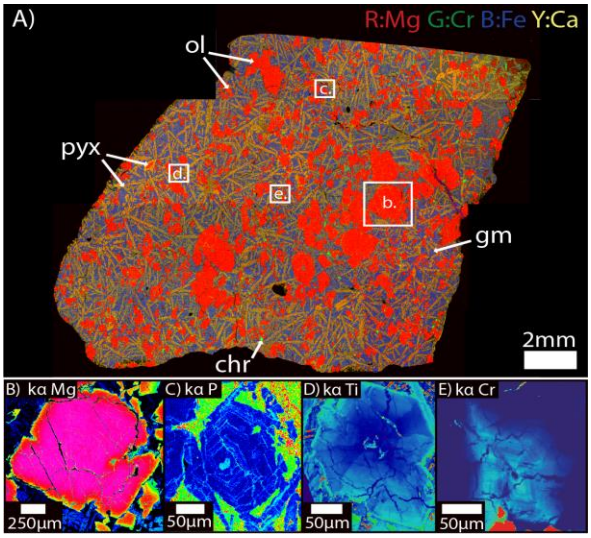

Figure 1: *A) Composite elemental x-ray mosaic of NWA8632 of Red:Mg, Green:Cr, Blue:Fe, Yellow:Ca. B) Mg Kα x-ray map of group 1a olivine, showing normal zoning. C) P Kα x-ray map of group 1b olivine, showing P-oscillatory zoning. D) Ti Kα x-ray map of group 2a pyroxene, showing sector-zoning. E) Cr Kα x-ray map of 2a pyroxene, showing oscillatory zoning. ol=olivine, pyx=pyroxene, chr=chromite, gm=groundmass.*

Phosphorus Zoning: Previous studies [e.g., 7,8] have found that olivine P-oscillatory zonation can be dominated by diffusion-controlled growth at high supersaturation, where an initial and rapid dendritic stage of primary and secondary branches are enriched in incompatible P followed by a period of slower growth

(Fig. 2). Group 1b olivine exhibit a "feathery" [8] P-rich pattern in the cores and mantles (Fig. 1C) that may be indicative of such growth induced by conductive cooling from the surrounding wall-rock in an enclosed magmatic chamber [7]. Group 1c olivine have P-enrichment in their skeletal structure that may correlate with a kinetic-controlled growth at disequilibrium conditions that rapidly "solute" trapped P [8].

Sector-Zoning: Recent work [10] has found that sector-zoning can occur from low-degrees of undercooling (ΔT) at near-equilibrium conditions. Similar to the "feathery" P-rich zones in olivine, sector-zoned grains may have an initial, rapid dendritic growth stage of primary and secondary branches dominated by diffusion-controlled growth [11], that sets the framework for the hourglass and prism sectors. Group 2a pyroxenes have defined hourglass sectors [5] and large, euhedral crystal habits supporting a period of slow growth that occurred after an initial, rapid dendritic stage (Fig. 2). Low-degree ΔT at near-equilibrium conditions sufficient enough to influence the rapid growth stage could be explained by conductive cooling of a magma chamber or potentially, chamber convection where melt interacts via a temperature gradient [12].

Magma Plumbing System: The olivine and pyroxene sub-groups are useful for placing constraints on the evolving crystallization conditions NWA 8632 experienced (Fig. 2). The texture, size, and chemistry of these grains suggest a 4-stage cooling history. Stage 1: group 1a olivine macrocrysts (Cores= Mg# 72.5) crystallized first, under equilibrium based on $K_d^{Fe\text{-}Mg}{}_{ol\text{-}melt}$ with the bulk-rock (Mg# 44.36). Stage 2: The onset of 1b olivine and euhedral group 2a pyroxenes suggests conductive cooling of the magma chamber that initiated the rapid dendritic growth stages. The oscillatory zoning of minor elements, such as Cr, in the pyroxene may be recording the onset of ascent for the sample [10] (stage 3) or chamber convection. Stage 3: the onset of group 2b elongated pyroxene crystallization suggests increased degrees of undercooling and disequilibrium growth at faster crystallization rates, e.g., crystallization in a conduit during ascent to the surface. Stage 4: Group 1c skeletal olivine and 2c dendritic pyroxene most likely crystallized near the lunar surface.

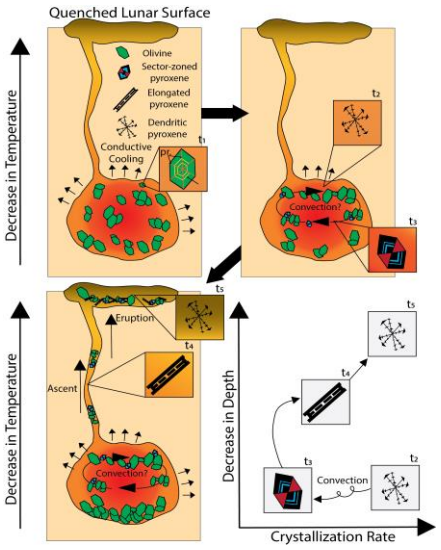

Figure 2: *Proposed magmatic evolution of NWA 8632 based on chemistry, size, and texture of olivine and pyroxenes.*

Comparison to other young, mare basalts: Previous studies suggested NWA 8632 may be launch-paired with a group of young, mare basaltic meteorites called the North-North-Lapaz (NNL) clan, consisting of NWAs 032, 4734, and Lapaz (LAP) 02205 group and potentially NWA 12008 [12]. Mineral zonation patterns (Fig. 1) and trace element chemistry of NWA 8632 are distinct from that of the NNL Clan (Fig. 3) [13], suggesting dissimilar magmatic histories. Nevertheless, they may sample different magmatic suites within the same volcanic region similar to the Apollo 12 and 15 basaltic sample suites [3].

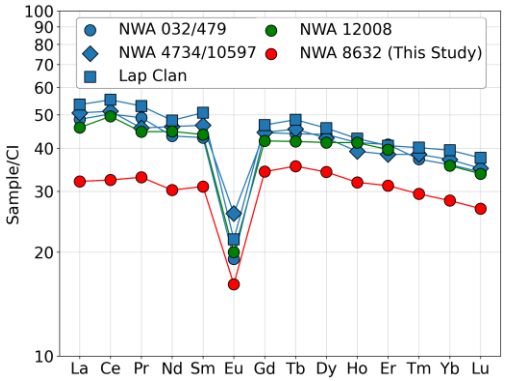

Figure 3: *REE plot of NWA 8632 (red) compared to young, basaltic meteorites of the NNL Clan (blue) and NWA 12008 (green) [14].*

Conclusion: NWA 8632 holds a critical record of late-mare volcanic activity on the Moon. To place further constraints on NWA 8632's magmatic evolution, we will examine any potential petrofabric by electron backscattered diffraction (EBSD) analysis, calculate diffusion and crystallization rates, and investigate this sample's parental magma genesis.

Acknowledgements: This project was funded by the NASA Grant#: 80NSSC19K0558, awarded to J. Gross.

References: [1] Hiesinger et al. (2023) *Rev. Min. Geochem.* 89, 401-451; [2] Shearer et al. (2023) *Rev. Min. Geochem.* 89,147-206; [3] Joliff et al., (2006) *Rev. Min. Geochem.;* [4] Fagan et al. (2018) *49th LPSC*, #2584. [5] Madera et al. (2023) *86th MetSoc*, #6053. [6] Anders & Grevesse (1989) *GCA*, 53-1. [7] Welsch et al. (2014) *Geology*, 42, 739-765. [8] Milman-Barris et al. (2008) *Contrib. Min. Pet.*, 155, 739-765. [9] Bence & Papike (1971) *EPSL*, 10, 245-251. [10] Ubide et al. (2019) *GCA* 251, 265-283. [11] Welsch et al. (2015) *Contrib. Min. Pet.* 171, 6. [12] Korotev & Irving (2021) *MaPS*, 36, 206-240. [13] Elardo et al. (2014) *MaPS*, 49, 261-291. [14] Cohen et al. (2019) *50th LPSC*, #2508.